

Quantitative calculations of the excitonic energy spectra of semiconducting single-walled carbon nanotubes within a π -electron model

Zhendong Wang, Hongbo Zhao, and Sumit Mazumdar

Department of Physics, University of Arizona, Tucson, Arizona 85721, USA

(Dated: August 26, 2018)

Using Coulomb correlation parameters appropriate for π -conjugated polymers (PCPs), and a nearest neighbor hopping integral that is arrived at by fitting the energy spectra of three zigzag semiconducting single-walled carbon nanotubes (S-SWCNTs), we are able to determine quantitatively the exciton energies and exciton binding energies of 29 S-SWCNTs within a semiempirical π -electron Hamiltonian that has been widely used for PCPs. Our work establishes the existence of a deep and fundamental relationship between PCPs and S-SWCNTs.

PACS numbers: 73.22.-f, 71.35.Cc, 78.67.Ch

I. INTRODUCTION

The photophysics of semiconducting single-walled carbon nanotubes (S-SWCNTs) are of strong current interest because of their potential applications in optoelectronics.^{1,2} Recent theoretical works have emphasized the Coulomb-induced binding between the optically excited electron and hole in these systems.^{3,4,5,6,7,8,9} The excitonic energy spectra of S-SWCNTs are now understood qualitatively: there occur in these nanotubes a series of energy manifolds labeled by an index $n = 1, 2, \dots$ etc., with each manifold containing both optically allowed and dark exciton states, and a continuum band separated from the optical exciton by a characteristic exciton binding energy. Nonlinear optical absorption measurements have demonstrated that distinct energy gaps occur between the lowest two-photon allowed states and the $n = 1$ optical excitons.^{10,11,12,13} This energy gap is a lower bound to the binding energy of the $n = 1$ optical exciton.¹³ Nonlinear absorption measurements involving the $n = 1$ continuum band¹⁴ and the $n = 2$ exciton¹⁵ have also been performed.

Exciton formation in S-SWCNTs is a consequence of direct Coulomb electron-electron (e-e) interaction, taking proper account of which is a notoriously difficult many-body problem. Theoretical calculations of excitons and continuum band energies in the S-SWCNTs are therefore necessarily approximate. One semiquantitative approach that has been popular employs an *ab initio* approach for the ground state, which is followed by the determination of the quasiparticle energies within the GW approximation and the solution of the Bethe-Salpeter equation of the two-particle Green's function.^{7,8} This approach becomes difficult to implement for chiral S-SWCNTs with large diameters and large unit cells, precisely the systems for which the nonlinear optical measurements are being performed.^{10,11,12,13,14,15} Scaling relationships for the exciton binding energies in wider chiral nanotubes have therefore been proposed.^{6,9} Understanding nonlinear absorption within such indirect approaches is difficult.

An alternate approach to the exciton problem in

the S-SWCNTs is to adopt a semiempirical π -electron approximation¹⁶ that is widely used to describe *planar* π -conjugated systems. The model assumes that the lowest energy excitations in planar conjugated systems involves the π -electrons only and ignores the electrons occupying orthogonal σ -bands. Since $\pi-\pi^*$ excitation energies decrease rapidly with increasing system size, while the σ and σ^* bands are nearly dispersionless, the approximation is excellent for large systems. Thus π -conjugated polymers (PCPs) have been discussed extensively within the semiempirical Pariser-Parr-Pople (PPP) Hamiltonian,¹⁶

$$H = - \sum_{\langle ij \rangle, \sigma} t_{ij} (c_{i\sigma}^\dagger c_{j\sigma} + c_{j\sigma}^\dagger c_{i\sigma}) + U \sum_i n_{i\uparrow} n_{i\downarrow} + \frac{1}{2} \sum_{i \neq j} V_{ij} (n_i - 1)(n_j - 1). \quad (1)$$

Here $c_{i\sigma}^\dagger$ creates a π -electron with spin σ (\uparrow, \downarrow) in the p_z orbital of the i th carbon atom, $\langle ij \rangle$ implies nearest neighbor (n.n.) atoms i and j , $n_{i\sigma} = c_{i\sigma}^\dagger c_{i\sigma}$ is the number of π -electrons with spin σ on the atom i , and $n_i = \sum_\sigma$ is the total number of π -electrons on the atom. The parameter t_{ij} is the one-electron hopping integral between p_z orbitals of n.n. carbon atoms, U is the on-site e-e repulsion between two π -electrons occupying the same carbon atom p_z orbital, and V_{ij} is the intersite e-e interaction.

The semiempirical model suffers from the disadvantage that determination of the parameters is commonly difficult. On the other hand, many-body problems that would be formidable within the *ab initio* approach, such as the enhancement of the ground state bond-alternation in polyacetylene by e-e interactions,¹⁷ or the occurrence of the lowest two-photon state below the optical state in finite polyenes and polyacetylene,¹⁸ can be understood within Eq. (1). The semiempirical approach should thus be taken as complementary to the *ab initio* one.

The above observations were the basis of our calculations within Eq. (1) of the electronic structures and exciton binding energies,⁵ and more recently, nonlinear optical absorptions¹³ in a limited number of S-SWCNTs, in spite of their nonplanarity. Justification of this procedure

can also be found in earlier work claiming that curvature effects of fullerene molecules can be included within Eq. (1) by proper modifications of the parameters.¹⁹ The e-e interaction and hopping integral parameters used in our calculations were the same ones that had been used earlier for the PCP poly-paraphenylenevinylene (PPV).²⁰ The calculated energy differences (~ 0.3 – 0.4 eV) between dominant two-photon states observed in ultrafast spectroscopy and the $n = 1$ optical excitons, in S-SWCNTs with diameters $d \geq 0.8$ nm, were remarkably close to what are observed experimentally.¹³ Other experimental work^{10,11,12,14} have also determined the binding energy of the $n = 1$ optical exciton in S-SWCNTs with diameters 0.8–1.0 nm to be ~ 0.4 eV, in agreement with Ref. 5. Very recent work has also confirmed the predicted binding energy of the $n = 2$ exciton in two different S-SWCNTs.¹⁵

The calculated *absolute energies* of the $n = 1$ and 2 excitons S-SWCNTs in our earlier work,^{5,13} however, are much larger than the experimental values (by as much as 0.5 eV). Equally importantly, comparisons of experimental and calculated exciton binding energies were based on considerations of diameters alone: while the nanotubes probed experimentally are chiral with large diameters, the theoretical calculations were either for zigzag nanotubes or for narrow chiral nanotubes, both with smaller unit cells. Direct comparisons of theory and experiment for the same systems were thus not possible. Finally, because the theoretical calculations could be performed for only a handful of nanotubes, family relationships, established experimentally,²¹ could not be demonstrated within the theoretical model.

In the present paper, we report calculated energy spectra of 29 S-SWCNTs, only 9 of which are zigzag, within Eq. (1). The diameters of the S-SWCNTs we consider range from 0.56 to 1.51 nm. These calculations have been possible because of substantive improvements in our computational techniques, while the improved results are a consequence of careful parametrization of the n.n. hopping integral $t_{ij} = t$ that takes into account curvature effects (see below). For each S-SWCNT we calculate the absolute energies E_{11} and E_{22} of the $n = 1$ and 2 optical excitons, and their binding energies E_{b1} and E_{b2} , respectively. We compare all theoretical quantities to experimentally determined ones.^{10,11,12,13,14,15,21,22,23} The large number of S-SWCNTs that could be considered allows us to investigate family relationships based on calculations of the energy ratio E_{22}/E_{11} and to compare these data to experiments.²¹ We find excellent agreement between the theory and experiments. Our work demonstrates convincingly that the photophysics of S-SWCNTs and PCPs can be understood within the same general theoretical framework, albeit with different hopping integrals.

TABLE I: Calculated and experimental (Ref. 22) $n = 1$ and 2 exciton energies for three zigzag S-SWCNTs.

(n,m)	t (eV)	E_{11} (eV)		E_{22} (eV)	
		SCI	Expt.	SCI	Expt.
(10,0)	1.8	1.10	1.07	1.97	2.31
	1.9	1.14		2.05	
	2.0	1.18		2.13	
	2.4	1.33		2.45	
(13,0)	1.8	0.90	0.90	1.59	1.83
	1.9	0.93		1.65	
	2.0	0.96		1.71	
	2.4	1.08		1.96	
(17,0)	1.8	0.73	0.80	1.24	1.26
	1.9	0.75		1.28	
	2.0	0.77		1.32	
	2.4	0.87		1.50	

II. METHOD AND PARAMETRIZATION OF π -ELECTRON MODEL

We use the single configuration interaction (SCI) approximation to compute the energies of the one electron-one hole excitations of the Hamiltonian in Eq. (1). The SCI approximation includes configuration mixings only between excitations that are singly excited from the Hartree-Fock (HF) ground state. The justifications for the approximation have been given before.^{5,13}

We discuss next how the parametrizations within Eq. (1) were reached. Since e-e interactions depend only on the distance and not on the curvature of the S-SWCNTs, it is logical to parametrize the V_{ij} exactly as in the PCPs,²⁰ viz.,

$$V_{ij} = \frac{U}{\kappa \sqrt{1 + 0.6117 R_{ij}^2}}, \quad (2)$$

where R_{ij} is the distance between carbon atoms i and j in Å. The two free parameters in Eq. (2) are U and κ ; the latter is introduced to take into account the dielectric screening due to the medium.²⁰ $U = 11.26$ eV and $\kappa = 1$ correspond to the standard Ohno parametrization for finite molecules.²⁴ SCI calculations of the optical absorption in PPV with five different U (between 0 to 10 eV) and three different κ (1, 2, and 3) had indicated that only with $U = 8$ eV and $\kappa = 2$ was it possible to fit all four absorption bands at 2.4, 3.7, 4.7, and 6.0 eV in PPV. The same U and κ were then used for quantitative calculations of nonlinear and triplet absorptions in PPV. Experimentally determined energies of the two-photon state that dominates nonlinear optical spectroscopy²⁵ and the lowest triplet state²⁶ agreed remarkably well with the theory. We have used the same U and κ for S-SWCNTs.

In the absence of any known procedure for determining t in S-SWCNTs, we had earlier^{5,13} chosen the value

2.4 eV that is used for planar aromatic systems.²⁷ Curvature in the S-SWCNTs implies smaller π - π overlap between n.n. C atoms and hence a smaller t . We arrive at the proper t by fitting the calculated E_{11} and E_{22} for three different zigzag nanotubes, (10,0), (13,0) and (17,0), against the corresponding experimental quantities (see below for discussions of how the experimental quantities were arrived at by previous authors). The theoretical exciton energies are for $U = 8$ eV and $\kappa = 2$, and four different $t = 1.8, 1.9, 2.0$, and 2.4 eV. Our results are summarized in Table I, which clearly indicates that $t = 2.4$ eV is too large and considerably better fits are obtained with $t = 1.8$ –2.0 eV. We have chosen $t = 2.0$ eV for the complete set of calculations we report below. The fits in Table I improve with increasing nanotube diameter, implying that strictly speaking the hopping integral is diameter-dependent even within the range of diameters we consider. We do not attempt further fine tuning of parameters as this would necessarily lead to loss of simplicity and generality.

As in previous work,^{5,13} we use open boundary condition (OBC). Surface states due to dangling bonds at the nanotube ends appear in the HF band structure, and are discarded at the SCI stage of our calculations. The chiral S-SWCNTs we investigate have gigantic unit cells. The number of unit cells we retain depend both on the size of the unit cell and the convergence behavior of E_{11} . The procedure involved calculating the standard tight-binding (TB) band-structure with periodic boundary condition (PBC), and then comparing the PBC E_{11} with that obtained using OBC with a small number of unit cells. The number of unit cells in the OBC calculation is now progressively increased until the difference in the computed E_{11} between OBC and PBC is less than 0.004 eV (worst case). It is with this system size that the SCI calculations are now performed using OBC. Thus for example, our calculations for (7,0), (6,4), and (7,5) SWCNTs are for 70, 16, and 5 unit cells, respectively, containing 1960, 2432, and 2180 carbon atoms, respectively. Since energy convergences are faster in the calculations with nonzero e-e interactions than the calculations in the TB limit, we are confident that this procedure gives accurate results. We retain an active space of 100 valence and conduction band states each in the SCI calculations. Stringent convergence tests involving gradual increase in the size of the active space indicate that the computational errors due to the energy cutoff is less than 0.005 eV (worst case). In addition to E_{11} and E_{22} we also calculate the corresponding exciton binding energies E_{b1} and E_{b2} , with the $n = 1$ and 2 continuum band threshold energies defined within the SCI to be the corresponding HF gaps.

III. RESULTS AND DISCUSSION

In Table II we have listed our calculated E_{11} , E_{22} , E_{b1} , and E_{b2} for 29 S-SWCNTs. We compare each

of these quantities to those obtained by experimental investigators.^{11,14,15,21,22,23} Nearly half the exciton energies listed in Table II as experimental were obtained directly from spectrofluometric measurements²¹ or from resonant Raman spectroscopy.²³ Using the experimental data in Ref. 21, Weisman and Bachilo²² derived empirical equations for the exciton energies of nanotubes for which direct experimental information do not exist. The experimental E_{11} and E_{22} in Table I are obtained from these empirical equations. Dukovic *et al.*¹¹ have given an empirical equation for the binding energy of the $n = 1$ exciton, which was also derived by fitting the set of E_{b1} obtained from direct measurements. Only two measured values exist currently for the binding energy of $n = 2$ exciton.¹⁵ We make distinctions between the experimental and empirical data in Table II, but in the text below we refer to both as experimental quantities. In Fig. 1 we have plotted the theoretical and experimental E_{11} and E_{22} against $1/d$, while in Fig. 1 inset we show the errors in our calculations, ΔE_{11} and ΔE_{22} , defined as the calculated energies minus the experimental quantities. As seen in the figure the theoretical plots are nearly independent of chirality, and depend primarily on diameter. This is a consequence of Eq. (1), within which the energetics depend only on the conductivity. We find excellent agreement between calculated and experimental E_{11} for $d > 0.75$ nm, with $|\Delta E_{11}| < 0.1$ eV. (The black arrow on the x-axis in Fig. 1 indicates $d = 0.75$ nm.) The agreement for $d > 1$ nm is even better with $|\Delta E_{11}| < 0.05$ eV. The larger disagreement with experiment (and the greater chirality dependency of the experimental energies) for $d < 0.75$ nm is due to the breakdown of the π -electron approximation. The disagreements between calculated and experimental E_{22} are larger, but even here the magnitude of the maximum error for $d > 0.75$ nm is within 0.2 eV, which is the C–C bond stretching frequency that can influence experimental estimation of exciton energies.⁹ The origin of the larger disagreement in the $n = 2$ region is the SCI approximation and not the π -electron model: inclusion of higher order CI is more important in general for higher energy states.

The agreement between the calculated and the experimental exciton binding energies in Table II is even more striking than the fits to the absolute energies. The discrepancies between theory and experiment is less than 10%, which is the uncertainty in the empirical binding energies.¹¹ Both E_{b1} and E_{b2} are inversely proportional to the diameter d and can be fitted approximately by

$$E_{b1} \simeq \frac{0.35}{d} \text{ eV}, \quad (3a)$$

$$E_{b2} \simeq \frac{0.42}{d} \text{ eV}. \quad (3b)$$

The exciton binding energies depend weakly on chirality. For both binding energies, the fits of Eq. (3) become better for larger diameter nanotubes. Eq. (3a) is remarkably close to the empirical formula $E_{b1} \simeq \frac{0.34}{d}$ eV given in previous experimental work.¹¹ Although there are not enough experimental data to verify the E_{b2} relation in Eq. (3b), the linear dependence against $1/d$ should be

TABLE II: Comparison of calculated and experimental/empirical $n = 1$ and 2 exciton energies and binding energies. The empirical exciton energies (Ref. 22) and exciton binding energies (Ref. 11) are in parentheses.

(n, m)	d (nm)	E_{11} (eV)		E_{22} (eV)		E_{b1} (eV)		E_{b2} (eV)	
		SCI	Expt. ^a	SCI	Expt.	SCI	Expt. ^c	SCI	Expt. ^d
(7,0)	0.56	1.58	(1.29)	2.92	(3.14)	0.56	(0.61)	0.79	
(6,2)	0.57	1.55	(1.39)	2.82	(2.96)	0.55	(0.59)	0.72	
(8,0)	0.64	1.44	(1.60)	2.38	(1.88)	0.56	(0.54)	0.57	
(7,2)	0.65	1.41	(1.55)	2.36	(1.98)	0.54	(0.52)	0.56	
(8,1)	0.68	1.34	(1.19)	2.45	(2.63)	0.48	(0.50)	0.65	
(6,4)	0.69	1.33	1.42	2.27	2.13 ^{a,b}	0.50	(0.49)	0.56	
(6,5)	0.76	1.24	1.27	2.15	2.19 ^{a,b}	0.45	0.43	0.54	
(9,1)	0.76	1.24	1.36	2.08	1.79 ^{a,b}	0.47	(0.45)	0.51	
(8,3)	0.78	1.21	1.30	2.05	1.87 ^a	0.45	0.42	0.50	
(10,0)	0.79	1.18	(1.07)	2.13	2.26 ^b	0.42	(0.43)	0.57	
(9,2)	0.81	1.17	(1.09)	2.10	2.24 ^b	0.42	(0.42)	0.55	
(7,5)	0.83	1.15	1.21	1.97	1.93 ^{a,b}	0.43	0.39	0.49	0.62±0.05
(8,4)	0.84	1.13	1.11	2.00	2.11 ^{a,b}	0.41	(0.40)	0.51	
(11,0)	0.87	1.11	(1.20)	1.86	(1.67)	0.42	(0.39)	0.46	
(10,2)	0.88	1.09	(1.18)	1.84	1.68 ^b	0.40	0.34	0.45	
(7,6)	0.90	1.08	1.11	1.88	1.92 ^{a,b}	0.39	0.35	0.47	
(9,4)	0.92	1.06	1.13	1.81	1.72 ^a , 2.03 ^b	0.39	0.34	0.44	
(11,1)	0.92	1.05	(0.98)	1.89	(2.03), 1.72 ^b	0.37	(0.37)	0.50	
(10,3)	0.94	1.03	0.99	1.84	1.96 ^{a,b}	0.37	(0.36)	0.48	0.49±0.05
(8,6)	0.97	1.01	1.06	1.75	1.73 ^{a,b}	0.37	0.35	0.44	
(13,0)	1.03	0.96	(0.90)	1.71	(1.83)	0.34	(0.33)	0.45	
(12,2)	1.04	0.95	0.90	1.69	1.81 ^a	0.33	(0.33)	0.44	
(10,5)	1.05	0.94	0.99	1.62	1.58 ^{a,b}	0.35	(0.32)	0.40	
(14,0)	1.11	0.91	(0.96)	1.54	(1.44)	0.34	(0.31)	0.38	
(12,4)	1.15	0.88	0.92	1.51	1.45 ^a	0.32	0.27	0.37	
(16,0)	1.27	0.81	(0.76)	1.44	(1.52)	0.28	(0.27)	0.37	
(17,0)	1.35	0.77	(0.80)	1.32	(1.26)	0.28	(0.25)	0.32	
(15,5)	1.43	0.73	(0.71)	1.29	(1.35)	0.25	(0.24)	0.32	
(19,0)	1.51	0.70	(0.66)	1.24	(1.30)	0.24	(0.23)	0.31	

^aFrom Ref. 21.

^bFrom Ref. 23.

^cFrom Ref. 11.

^dFrom Ref. 15.

true for both binding energies. The calculated E_{b1} and E_{b2} are very close to those obtained earlier by us for the wide nanotubes with $t = 2.4$ eV,^{5,13} even as the calculated E_{11} and E_{22} are now quite different. This is simply a consequence of localization of the electrons at the large U/t considered here: exciton binding energies in this case depend primarily on electron correlation. Recall, for example, that in the limit where the intersite Coulomb interaction is cut off beyond the n.n. interaction V_1 , the exciton binding energy is determined almost entirely by the difference in Coulomb interactions $U - V_1$,¹⁷ with t playing a weak role for $U/t \geq 4$.

Our ability to calculate E_{11} and E_{22} for a large number of nanotubes allows us to demonstrate family be-

havior within Eq. (1), which was not possible before. It has been shown that in plots of experimental E_{22}/E_{11} against the wavelength λ_{22} corresponding to E_{22} , families of (n, m) S-SWCNTs with the same $n - m$ lie on the same continuous curves.²¹ The experimental energy ratios diverge from a central limiting number ~ 1.75 , with the deviations increasing with $n - m$, and with the direction of the deviation being positive for the families $(n - m) \bmod 3 = 1$ and negative for the families $(n - m) \bmod 3 = 2$, respectively.²¹ In Fig. 2 we have plotted our calculated E_{22}/E_{11} against the calculated λ_{22} . The calculated ratios do not show the same smooth behavior as in Ref. 21, since as already noticed in Fig. 1 inset our errors with E_{22} are larger than those with E_{11} . Never-

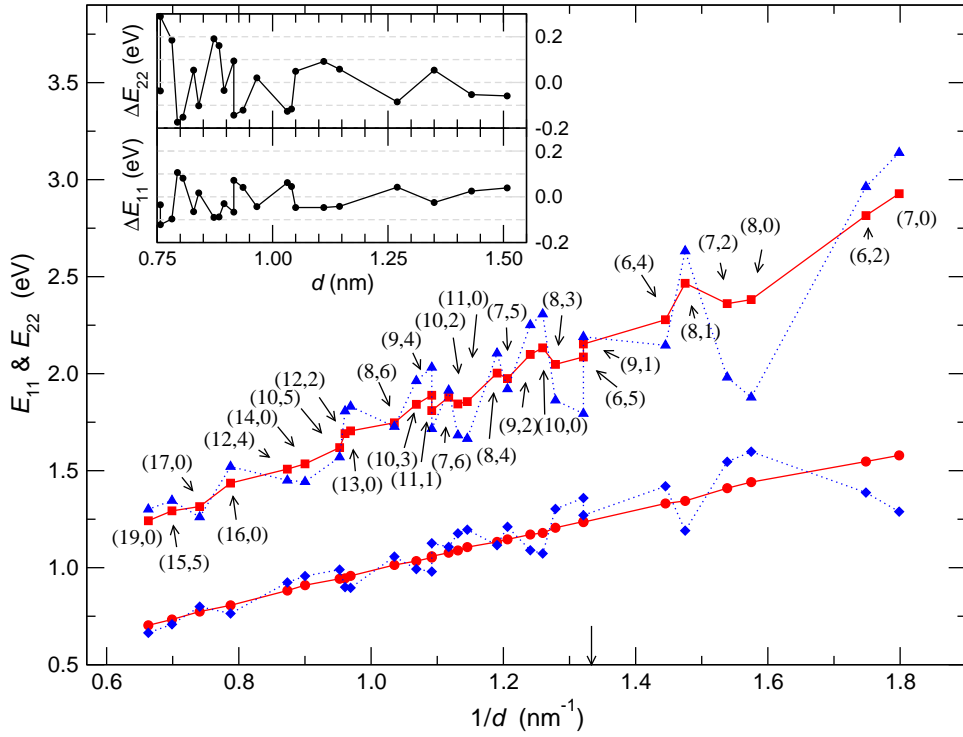


FIG. 1: (Color online) Calculated (red solid line, circle and square symbols) vs. experimental (blue dotted line, diamond and triangle symbols) E_{11} and E_{22} for 29 S-SWCNTs. The inset shows errors ΔE_{ii} ($i = 1, 2$) in the calculations, defined as the calculated minus the experimental or empirical energies.

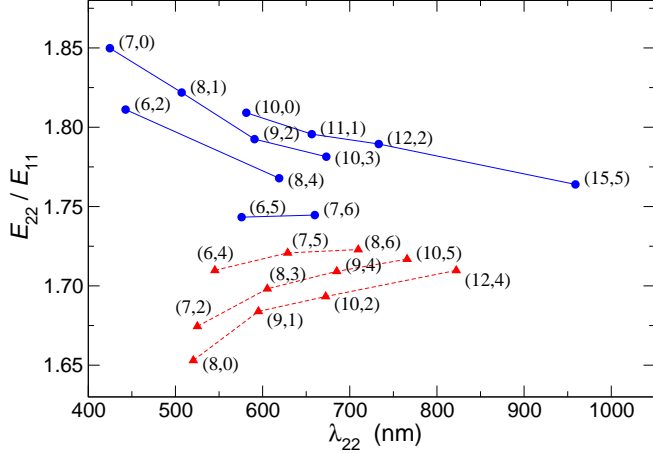


FIG. 2: (Color online) Calculated E_{22}/E_{11} vs. the wavelength λ_{22} corresponding to E_{22} . The blue solid line with circle symbols (red dashed line with triangle symbols) denote families $(n - m) \bmod 3 = 1$ (2).

theless, two different classes of behavior, for the families $(n - m) \bmod 3 = 1$ and $(n - m) \bmod 3 = 2$ are very clear. The difference between the largest and the smallest ratios in the narrow diameter (small λ_{22}) end is smaller than what is seen experimentally, but this is once again merely a consequence of the larger errors in our calculations for the narrower nanotubes. More importantly, the

limiting E_{22}/E_{11} in the wide diameter (large λ_{22}) end in Fig. 2 is very close to the experimental limiting ratio of 1.75.

IV. CONCLUSION

In summary, direct calculations of the energy spectra of a large number of S-SWCNTs within the π -electron PPP model Hamiltonian and with a fixed set of parameters show excellent agreement with experiments. The magnitudes of two of the three free parameters, U and κ for Coulomb interactions, are the same as those used earlier to calculate the energy spectrum of PPV,²⁰ the third free parameter t is obtained by fitting the energetics of three zigzag S-SWCNTs to account for the curvature effects. The calculated exciton energies and exciton binding energies in the first two manifolds are in excellent agreement with experiments, and the “family behavior” is demonstrated. In the diameter range of our calculated S-SWCNTs, we found linear dependence against $1/d$ for the binding energies of excitons in both manifolds. It is unlikely that the agreement between theory and experiments is fortuitous. The Coulomb parameters used here were obtained after extensive search through a very large parameter space for PPV, and the same parameters successfully reproduced the energies of the dominant two-photon state²⁵ and the triplet energy spectrum²⁶ of PPV.

Similarly, slightly smaller hopping in S-SWCNTs than in PPV is to be expected.¹⁹ Our work demonstrates a universality in the photophysics of S-SWCNTs and PCPs that arises from their common quasi-one-dimensionality and π -conjugation. The existing rich literature on the photo- and device physics of PCPs can therefore provide valuable guidance in the search for optoelectronic appli-

cations of S-SWCNTs.

Acknowledgments

This research was supported by NSF-DMR-0406604.

¹ J. A. Misewich, R. Martel, Ph. Avouris, J. C. Tsang, S. Heinze, and J. Tersoff, *Science* **300**, 783 (2003).

² T. Hertel and G. Moos, *Phys. Rev. Lett.* **84**, 5002 (2000).

³ T. Ando, *J. Phys. Soc. Jpn.* **66**, 1066 (1997).

⁴ M. F. Lin, *Phys. Rev. B* **62**, 13153 (2000).

⁵ H. Zhao and S. Mazumdar, *Phys. Rev. Lett.* **93**, 157402 (2004).

⁶ C. L. Kane and E. J. Mele, *Phys. Rev. Lett.* **90**, 207401 (2003); **93**, 197402 (2004).

⁷ C. D. Spataru, S. Ismail-Beigi, L. X. Benedict, and S. G. Louie, *Phys. Rev. Lett.* **92**, 077402 (2004); R. B. Capaz, C. D. Spataru, P. Tangney, M. L. Cohen, and S. G. Louie, *Phys. Rev. Lett.* **94**, 036801 (2005).

⁸ E. Chang, G. Bussi, A. Ruini, and E. Molinari, *Phys. Rev. Lett.* **92**, 196401 (2004).

⁹ V. Perebeinos, J. Tersoff, and Ph. Avouris, *Phys. Rev. Lett.* **92**, 257402 (2004); **94**, 027402 (2005).

¹⁰ F. Wang, G. Dukovic, L. E. Brus, and T. F. Heinz, *Science* **308**, 838 (2005).

¹¹ G. Dukovic, F. Wang, D. Song, M. Y. Sfeir, T. F. Heinz, and L. E. Brus, *Nano Lett.* **5**, 2314 (2005).

¹² J. Maultzsch, R. Pomraenke, S. Reich, E. Chang, D. Prezzi, A. Ruini, E. Molinari, M. S. Strano, C. Thomsen, and C. Lienau, *Phys. Rev. B* **72**, 241402(R) (2005).

¹³ H. Zhao, S. Mazumdar, C.-X. Sheng, M. Tong, and Z. V. Vardeny, *Phys. Rev. B* **73**, 075403 (2006).

¹⁴ Y.-Z. Ma, L. Valkunas, S. M. Bachilo, and G. R. Fleming, *J. Phys. Chem. B* **109**, 15671 (2005).

¹⁵ Z. Wang, H. Pedrosa, T. Krauss, and L. Rothberg, *Phys. Rev. Lett.* **96**, 047403 (2006).

¹⁶ R. Pariser, and R. G. Parr, *J. Chem. Phys.* **21**, 466 (1953); J. A. Pople, *Trans. Faraday Soc.* **49**, 1375 (1953).

¹⁷ D. Baeriswyl, D. K. Campbell, and S. Mazumdar, in *Conjugated Conducting Polymers*, edited by H. Kiess (Springer-Verlag, Berlin, 1992).

¹⁸ Z. G. Soos, S. Ramasesha, and D. S. Galvão, *Phys. Rev. Lett.* **71**, 1609 (1993).

¹⁹ R. C. Haddon, *Science* **261**, 1545 (1993).

²⁰ M. Chandross, S. Mazumdar, M. Liess, P. A. Lane, Z. V. Vardeny, M. Hamaguchi, and K. Yoshino, *Phys. Rev. B* **55**, 1486 (1997); M. Chandross and S. Mazumdar, *Phys. Rev. B* **55**, 1497 (1997).

²¹ S. M. Bachilo, M. S. Strano, C. Kittrell, R. H. Hauge, R. E. Smalley, and R. B. Weisman, *Science* **298**, 2361 (2002).

²² R. B. Weisman and S. M. Bachilo, *Nano Lett.* **3**, 1235 (2003).

²³ C. Fantini, A. Jorio, M. Souza, M. S. Strano, M. S. Dresselhaus, and M. A. Pimenta, *Phys. Rev. Lett.* **93**, 147406 (2004).

²⁴ K. Ohno, *Theor. Chim. Acta* **2**, 219 (1964).

²⁵ S. V. Frolov, Z. Bao, M. Wohlgemant, and Z. V. Vardeny, *Phys. Rev. Lett.* **85**, 2196 (2000).

²⁶ A. P. Monkman, H. D. Burrows, M. D. Miguel, I. Hamblett, and S. Navaratnam, *Chem. Phys. Lett.* **307**, 303 (1999).

²⁷ L. Salem, *The molecular orbital theory of conjugated systems* (Benjamin, New York, 1966).